Energy and exergy analysis of a cruise ship

Francesco Baldi[a], Fredrik Ahlgren[b], Tuong-Van Nguyen[c], Cecilia Gabrielii[d],
Karin Andersson[d]

[a]*Industrial Process Energy Systems Engineering (IPESE), École Polytechnique Fédérale
de Lausanne, 1950, Sion, Switzerland*
[b]*Kalmar Maritime Academy, Linnaeus University, Kalmar, Sweden*
[c]*Department of Mechanical Engineering, Technical University of Denmark, Lyngby,
Denmark*
[d]*Department of Mechanics and Maritime Sciences, Chalmers University of technology,
Gothenburg, Sweden*

Abstract

Keywords:
low carbon shipping, energy analysis, exergy analysis, energy efficiency

1. Introduction

1.1. Background

CO₂ emissions from shipping in 2012 amounted to a total of 949 million tonnes, contributing to 2.7% of global anthropogenic CO_2 emissions [1]. Although this contribution appears relatively low, the trend is that shipping will play an even greater role in the future due to the increased transport demand according to all IMO future scenarios [1]. As an example, global transport demand has increased by 3.4% in 2014, compared to a global GBP growth of 2.5% the same year, which shows how shipping tends to rise even faster than global economy [2]. The OECD countries have reduced the CO_2 impact from shipping, but a larger amount has been moved to the non-OECD countries [3]. The fact that shipping needs to even further reduce its CO_2 emissions in the near future is essential for being able to achieve the goals of maintaining the climate below a 2-degree level in 2050 [4].

In addition to considerations related to GHG emissions, an emission control area (ECA) is enforced in the Baltic Sea by the International Maritime Organisation since January 2015. This ECA stipulates that the fuel used must not contain more than 0.1% sulphur, therefore requiring the use of

more expensive distillate fuels. More generally making shipping sustainable is a challenge that will demand growing attention by the shipping industry [3]

Altogether, these conditions present a challenge to the shipping companies who attempt to reduce their fuel consumption, environmental impact, and operative costs. A wide range of fuel saving solutions for shipping are available and partially implemented in the existing fleet, both from the design and operational perspective; several specific studies have been conducted on these technologies, and a more detailed treatise would be out of the scope of this work. In this context, it has been acknowledged that the world fleet is heterogeneous, and measures need to be evaluated on a ship-to-ship basis [4]. In this process, a deeper understanding of energy use on board of the specific ship is vital.

1.2. Previous work

The idea of improving the understanding of the behavior of the energy system of a ship is not new. Most of the work published around this subject relates to the use of mathematical models of the ship systems.

Most authors focused on the propulsion part of the problem, as this is often the most relevant energy demand on board. Shi et al. proposed a modeling approach for predicting ship fuel consumption of a cargo/passenger ferry [5]; Theotokoats and Tzelepis applied a similar procedure to the case of a Handymax product carrier [6], similarly to Tillig et al., who also added the dynamic element to their predictive model [7].

The work referenced above allowed improving the understanding of how many operational (such as the ship's speed) and environmental (such as wave height and wind speed) parameters influence the ship's energy performance. These studies, however, are not based on actual measurements of the ship's operations. Also, they focus entirely on the ship's power demand for propulsion. This is a very reasonable practice for most ship types, given that propulsion represent the largest part of the total energy demand, but does not allow improving the knowledge of the remaining part of the system.

Other authors filled the gap by both including electric energy demand, and by basing their work on measurements from actual ship operations. The work presented by Thomas et al. [8] and Basurko et al. [9] shows the application of energy auditing methods to fishing vessels. This approach represents a step forward towards improving the understanding of how energy is used on board during actual ship operations.

More generally, several authors have highlighted the importance of a detailed knowledge of the ship's operational profile in order to appropriately assess and optimize possible alternatives for improving ship energy efficiency [10]. Coraddu et al., started from a statistical analysis of measured ship operations and used the aggregated data, together with a computational model of the vessel, to provide a better prediction of the actual ship's operational efficiency [11]. The importance of considering the operational profile was also showed in the case of the optimization of engine-propeller interaction [12], in the process of retrofitting existing systems [13, 14], and in ship design [15, 16].

Heat demand is rarely a subject of concern on board ships, with some notable exceptions. This is due to a combination of generally low demand and high availability from the waste heat of the engines. In a previous publications by the authors, for instance, it is shown that in the case of a product tanker, although the heat demand was estimated to account for roughly 20% of the total energy demand of the ship on a yearly basis, it only contributes to 4.1% of the total fuel consumption (contribution of the auxiliary boilers), while the rest of the demand is fulfilled using waste heat [17].

It should be noted that, however, much research effort has been devoted, especially in recent times, to the improvement of the efficiency of ship energy systems by recovering the waste heat available from the engines. With reference to different types of technologies, case studies, and designs,the several authors showed the existance of a quite significant potential for energy saving when WHR systems are employed, ranging from around 1% for single-pressure steam cycles applied to two-stroke engines [18] to more complex systems based on ORCs (up to 10%, [19]) or including the cooling systems as a source of waste heat (over10%, [20]). The case of the installation of an ORC on board of the vessel investigated in this study (see Section 2.2) was presented in [21], showing a similar potential.

The potential uses for waste heat on board are not limited to improving the efficiency of the power plant. Waste heat is commonly used for fulfilling on board heat demand for spatial heating and freshwater generation [22, 17, 23]; Balaji et al. proposed the use of waste heat for ballast-water systems [24]; Salmi et al. suggested its use for adsorption refrigeration systems [25]. A detailed review of potential uses for waste heat from marine engines is presented by Shu et al [26].

Some ship types constitute notable examples. On cruise ships the heat demand is significantly higher compared to standard cargo ships. Referring

to winter conditions, Marty et al. estimated the instantaneous heat demand of a selected cruise ship to reach roughly 23 MW, compared to an estimated peak of 49 MW for propulsion and electric auxiliaries combined [27].

This shows how the heat from the engines should be considered as a potential resource, rather than a waste, and that there is potential for improvement based on the optimal use of these heat sources. The work presented by the authors in [28] represent a step in this direction; however, there is the need for an increased detail in the estimation of the heat demand.

Exergy analysis provides a more accurate estimation of the potential for energy recovery on board. The application of exergy analysis to the case of ship energy systems is, however, still limited. Dimopoulos et al. showed how the process optimizing the WHR system of a container ship can be more efficient if exergy efficiency, rather than energy efficiency, is used as the target of the optimization [20]; Baldi et al. also analyzed the exergy flows on board of a product tanker, showing that this allows having a more accurate understanding of what parts of the system show potential for improvement [17]; similar results were obtained by Marty et al., who focused on the power plant of a cruise ship [29]. Koroglu et al. made a step futher also including advanced exergy analysis in their study [30].

1.3. Aim

Given the existing limitations of the current available information in scientific literature highlighted in the previous section, the objective of this work is the following:

- Analyse the demand of a cruise ship in terms of propulsion power, electric power and heat, based on operational measurements. The lack of existing information with reference to the heat demand is considered a particular element of novelty when compared to existing literature in the subject.

- Analyse the current efficiency of the system, and potential ways to improve it, by means of applying exergy analysis.

- Provide reference operational conditions for further use in the field of energy systems optimization.

4

2. Method

In this paper, we present the application of energy and exergy analysis (described in section 2.1) to a cruise ship. This is done for one specific case study vessel, that is described in detail in Section 2.2; in Section 2.3 we present the specifics of the available information, in particular the measured data and the technical documentation; the specific assumptions and methods used for processing the available information into energy and exergy flows are specified in Section 2.4. In these regards, the estimation of the heat demand is treated in a separate section (Sec. 2.6) as it constitutes a particularly challenging task and it is one of the central aspects of this article.

2.1. Energy and exergy analysis

2.1.1. Energy analysis

Energy can be stored, transformed from one form to another (e.g. heat to power) and transferred between systems, but can neither be created nor destroyed (conservation law) **Bejan et al.**. The system under study is the *ship energy system* and is thus taken as control volume. The energy balance can be expressed as:

$$\sum_{\text{in}} \dot{H}_{\text{in}} = \sum_{\text{out}} \dot{H}_{\text{out}} \tag{1}$$

$$\dot{H}_{\text{fuel}} + \dot{H}_{\text{air}} = \sum_{\text{waste}} \dot{H}_{\text{waste}} + \dot{W}_{\text{el}} + \dot{Q}_{\text{heating}} \tag{2}$$

The left-hand side term represents, on a time rate basis, the energy associated with the fuel consumed in the boilers and engines ($\dot{H}_{\text{fuel}}$) and the air used in the combustion processes ($\dot{H}_{\text{air}}$). The right-hand side term denotes the power ($\dot{W}_{\text{el}}$) and heat ($\dot{Q}_{\text{heating}}$) required on-site (e.g. propulsion and fuel heating), and the heat discharged into the environment ($\sum_{\text{waste}} \dot{H}_{\text{waste}}$) with, for instance, the exhaust gases.

The energy flow associated with a material stream is calculated as the sum of the physical and chemical enthalpies, and kinetic and potential energies are neglected. The physical energy is taken as the relative enthalpy, as underlined in **Kotas et al.**, and the chemical energy is taken as the lower/higher heating value. The environmental conditions taken for the present analysis are the ambient pressure and seawater temperature.

2.1.2. Exergy analysis

Exergy may be defined as the 'maximum theoretical useful work (shaft work or electrical work) as the system is brought into complete thermodynamic equilibrium with the thermodynamic environment while the system interacts with it only' [**?**]. Unlike energy, exergy is not conserved but some is destroyed because of the irreversible phenomena taking place in real processes (e.g. chemical reactions like combustion). The exergy balance for the system under study can be expressed as:

$$\sum_{\text{in}} \dot{E}_{\text{in}} = \sum_{\text{out}} \dot{E}_{\text{out}} + \dot{E}_d \tag{3}$$

$$\dot{E}_{\text{fuel}} + \dot{E}_{\text{air}} = \sum_{\text{waste}} \dot{E}_{\text{waste}} + \dot{E}_W + \dot{E}_{Q,\text{heating}} + \dot{E}_d \tag{4}$$

The left-hand side term represents, on a time rate basis, the exergy associated with the fuel and air. The right-hand side term denotes the exergy of the waste streams, the exergy transfers with heat and power, and the exergy destroyed in the ship system. Kinetic and potential exergies are neglected, and the exergy of a given material stream is derived as the sum of the physical and chemical exergies. The chemical exergy is calculated based on the reference environment of **Szargut (1989)**, and its value is approximatively equal to the higher heating value for hydrocarbon fuels. The exergy destruction can be calculated from the Gouy-Stodola theorem :Kotas (1995).

The exergy balance may alternatively be formulated as:

$$\dot{E}_{\text{p}} = \dot{E}_{\text{f}} - \dot{E}_{\text{d}} - \dot{E}_{\text{l}} \tag{5}$$

where $\dot{E}_{\text{p}}$ is called the exergy product, and corresponds to the desired output of the system, in exergy terms (for example, the power produced in an engine). $\dot{E}_{\text{f}}$ denotes the exergy fuel, and represents the resources spent to drive the studied process (for instance, the fuel used in a combustion process). The last term $\dot{E}_{\text{l}}$ corresponds to the losses of a system, such as the heat discharged into the environment with cooling water.

2.1.3. System performance

The following indicators are used to evaluate the system performance:

- the exergy efficiency ε, defined as the ratio between the exergy product and fuel of a given component or system

$$\varepsilon = \frac{\dot{E}_{\mathrm{p}}}{\dot{E}_{\mathrm{f}}} \qquad (6)$$

- the efficiency defect λ, presented in the work of Kotas, defined as the fraction of the total exergy input destroyed in the successive irreversible processes

$$\lambda = \frac{\dot{E}_{\mathrm{d}}}{\dot{E}_{\mathrm{in,tot}}} \qquad (7)$$

- the irreversibility share δ, suggested in the work of Tsatsaronis, defined as the ratio between the exergy destroyed in the i-th component in relation to the exergy destroyed in the entire system

$$\delta_i = \frac{\dot{E}_{\mathrm{d},i}}{\dot{E}_{\mathrm{d,tot}}} \qquad (8)$$

2.2. Case study vessel

The energy and exergy analysis are here applied to a specific cruise ship operating daily cruises in the Baltic Sea between Stockholm and the island of Åland. The ship is 176.9 m long and has a beam of 28.6 m, and has a design speed of 21 knots. The ship was built in Aker Finnyards, Raumo Finland in 2004.

The ship has a capacity of 1800 passengers and has several restaurants, night clubs and bars, as well as saunas and pools. This means that the energy system regarding the heat and electricity demand is more complex than a regular cargo vessel in the same size. Typical ship operations, although they can vary slightly between different days, are represented in Figure **??**. It should be noted that the ship stops and drifts in open sea during night hours before mooring at its destination in the morning, if allowed by weather conditions.

The ship systems are summarized in Figure **??**. The propulsion system is composed of two equal propulsion lines, each made of two engines, a gearbox, and a propeller. The main engines are four Wrtsil 4-stroke Diesel engines (ME) rated 5850 kW each. All engines are equipped with selective catalytic reactors (SCR) for NOX emissions abatement. Propulsion power is needed

whenever the ship is sailing; however, it should be noted that the ship rarely sails at full speed, and most of the time it only needs one or two engines operated simultaneously.

Auxiliary power is provided by four auxiliary engines (AE) rated 2760 kW each. Auxiliary power is needed on board for a number of alternative functions, from pumps in the engine room to lights, restaurants, ventilation and entertainment for the passengers.

Auxiliary heat needs are fulfilled by the exhaust gas steam generators (HRSG) located on all four AEs and on two of the four MEs or by oil-fired auxiliary boilers (mainly when in port, or during winter), by the heat recovery on the HT cooling water systems (HRHT), and by the auxiliary, oil fired boilers (AB). The heat is needed for passenger and crew accommodation, as well as for the heating of the highly viscous heavy fuel oil used for engines and boilers. This last part, however, is drastically reduced since the 1st of January 2015, as new regulations entering into force require the use of low-sulphur fuels, which require a much more limited heating.

2.3. Data gathering and pre-processing

The operational data was collected on board from the ships' machine logging and surveillance system. The on board database tool exported all logging points to Excel-97 files, and due to the extensive amount of data points the export was divided in to 15 individual Excel-files consisting of a total 665 MB. The exported raw-data from the ship was over a time span of a full year and in most data-points in 15-min average. The Excel-files were processed in the Pandas library which is a high performance data analysis tool in Python [31]. A new structured naming of headers and a consistent time frequency over all data points were created, and 245 selected data points were saved in a HDF5 table time series database which is the base for the analysis.

All data-points were checked individually by creating a descriptive statistic and a histogram of each data-point. A filter was applied by setting up a pre-defined maximum and minimum value. As we do not know, or had any meaningful way of deriving, each individual sensors placement, sensor type or calibration status all data must be filtered and checked accordingly for outliers or bad data.

Since measurements of ambient and seawater temperature from onboard logging systems were not available for the whole dataset, we used measurements taken from SMHI database for Landsort lighthouse for the sea-

water, and the lighthouse Svenska Högarna for the ambient temperature. The Landsord lighthouse is situated south of the Stockholm archipelago, and the Svenska Högarna lighthouse is along the ship route, in between the Swedish archipelago and land. The assumption was validated based on June-December period, for which onboard measurements were available. This resulted in a root mean square error of 1.5 K and 1.9 K for the seawater and the ambient temperature respectively, which we considered to be accurate enough for the purpose of this work. The fit the SMHI-data with the rest of the data-set the SMHI data was resampled from 1h for the seawater and 3h for the ambient temperature, to 15min frequency using a linear interpolation.

2.4. Data processing: Ship energy system modeling

Not all of the variables required to perform a full energy and exergy analysis of the system are available from measurements. In some cases, they are measurable, but not measured (e.g. some temperatures, mass flows, etc.). In other cases, they are simply impossible, or impractical, to measure (e.g. specific enthalpy, specific entropy). For this reason, part of the ship systems needed to be modeled in order to derive the unknown variables.

2.4.1. Diesel engines

The setup of the engines and their connections to the other ship systems are summarized in Figure 1 for the main and auxiliary engines, respectively. The most relevant operative values are provided in Tables 1 and 2 and the main energy flows are listed in Tables 3 and 4. It should be noted that, in the case of the main engines, the engine power output was not measured and needed to be estimated. In this work, we calculated the engine power output based on measurements of engine fuel rack position (used as a proxy of the mass of fuel injected per cycle) and of the engine speed:

$$\dot{m}_{fuel} = \dot{m}_{fuel,des}\left(a_0 + a_1\frac{frp}{frp_{des}}\right)\frac{\omega}{\omega_{des}} \tag{9}$$

$$\eta_{ME} = a_0 + a_1\frac{\dot{m}_{fuel}}{\dot{m}_{fuel,des}} + a_2\left(\frac{\dot{m}_{fuel}}{\dot{m}_{fuel,des}}\right)^2 \tag{10}$$

$$\dot{W}_{ME} = \dot{m}_{fuel}\eta_{ME}LHV \tag{11}$$

The validity of this assumption can be seen by observing Figures 2 and 3 where the calculated power from the main engines is represented against the ship speed and the turbocharger speed, respectively.
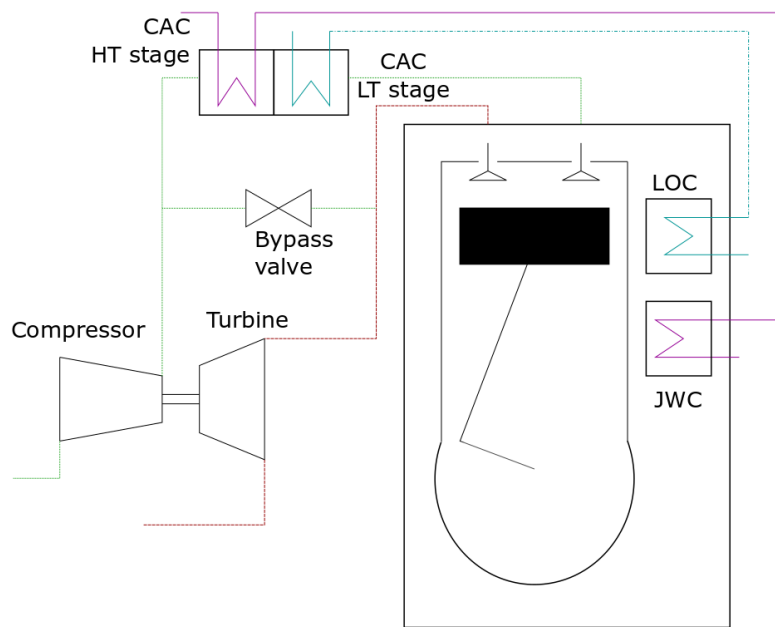
Figure 1: Schematic representation of the Diesel engines and their connections to the cooling systems
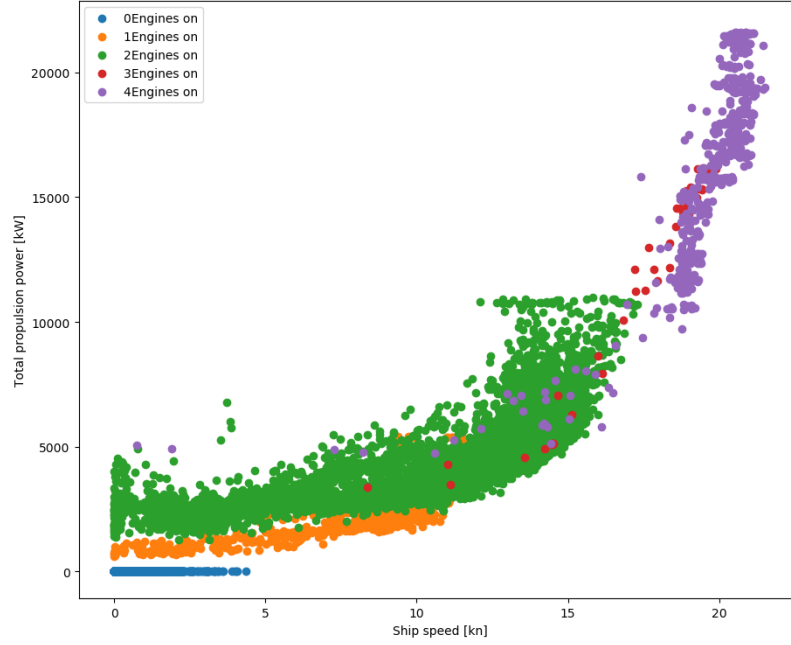
Figure 2: Scatter plot, Propulsion power versus ship speed

In the case of the auxiliary engines, instead, direct measurements of the power generated by each engine were available.

For both auxiliary and main engines, part of the relevant internal variables are not measured (particularly with relation to the bypass valves) and this required to determine them based on modeling the heat and mass balance of the engine. The model is explained in detail in Appendix REF.

INCLUDE VALIDATION AGAINST PROJECT GUIDE DATA
INCLUDE VALIDATION AGAINST PROJECT GUIDE DATA

2.4.2. Cooling systems

The ship's cooling systems are designed similarly to most ships and divided in two cooling systems of two separate temperature levels: the high temperature (HT) cooling systems (70-90°C) and the low temperature (LT) cooling systems (40-60°C). The cooling systems provide the necessary cooling to the engines, to the steam systems and to all other components on board.
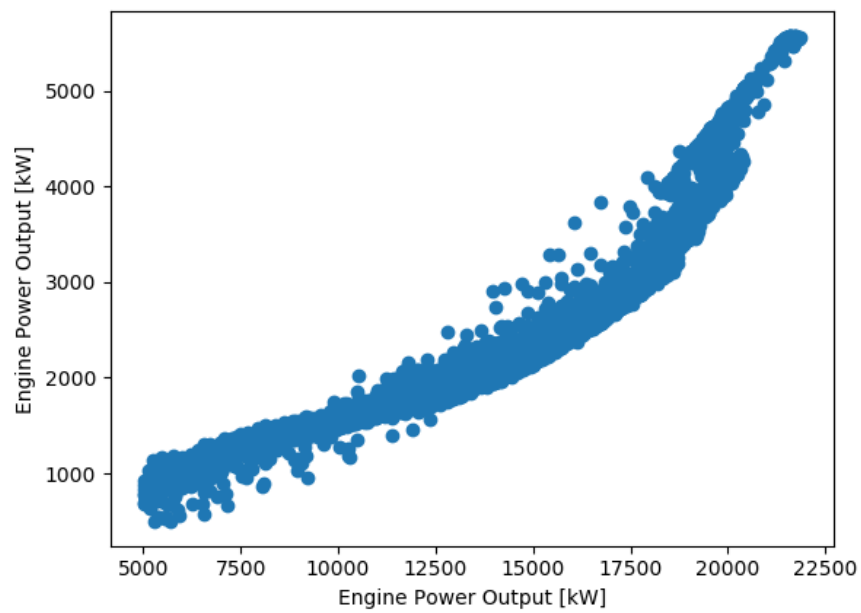
Figure 3: Scatter plot, Main engine power versus turbocharger speed (ME1)

Variable	Unit	M/C	30%	50%	70%	90%
Compressor						
$T_{air,in}$	^oC	M		302		
$T_{air,out}$	^oC	C	356.0	409.4	434.1	461.7
$\dot{m}_{air}$	kg/s	C	4.24	7.62	8.51	10.28
β_{comp}	-	M				
Turbine						
$T_{eg,in}$	^oC	C	698.8	702.2	763.3	786.0
$T_{eg,out}$	^oC	M	639.3	592.9	633.2	631.0
$\dot{m}_{eg}$	kg/s	C	4.35	7.79	8.73	10.57
β_{exp}	-	C				
Bypass valve						
$\dot{m}_{air,BP}$	kg/s	C	0.98	2.05	1.02	0.39
Cylinders						
$\dot{m}_{air,in}$	kg/s	C	3.25	5.57	7.49	9.89
$\dot{m}_{fuel,in}$	kg/s	C	0.11	0.17	0.22	0.28
$\dot{m}_{eg,out}$	kg/s	C	3.37	5.74	7.71	10.17
$T_{air,in}$	^oC	M	323.7	323.2	323.1	323.5
$T_{eg,out}$	^oC	M	698.8	702.2	763.3	786.0
CAC-LT stage						
$T_{air,in}$	^oC	C	355.2	350.1	360.0	368.7
$T_{air,out}$	^oC	M	323.7	323.2	323.1	323.5
$T_{w,in}$	^oC	M	309.3	309.6	309.5	309.6
$T_{w,out}$	^oC	C	310.4	311.0	311.8	313.0
$\dot{m}_{w,LT}$	kg/s	C	23.36	26.09	29.1	31.53
CAC-HT stage						
$T_{air,in}$	^oC	C	356.0	409.4	434.1	461.7
$T_{air,out}$	^oC	C	355.2	350.1	360.0	368.7
$T_{w,in}$	^oC	C	360.8	360.2	359.6	358.7
$T_{w,out}$	^oC	C	360.8	362.6	363.6	365.4
$\dot{m}_{w,HT}$	kg/s	C	33.21	33.18	33.33	33.33
LOC						
$T_{lo,in}$	^oC	C	346.6	348.9	349.8	350.5
$T_{lo,out}$	^oC	M	335.1	336.8	338.1	338.3
$T_{w,in}$	^oC	C	310.4	311.0	311.8	313.0
$T_{w,out}$	^oC	C	317.4	317.6	317.5	318.5
JWC						
T_{wall}	^oC	C		423		
$T_{w,in}$	^oC	M	358.1	358.4	357.6	356.4
$T_{w,out}$	^oC	C	360.8	360.2	359.6	358.7

Table 1: Main engines, measured and calculated temperatures and flows at different engine loads

Variable	Unit	M/C	30%	50%	70%	90%
Compressor						
$T_{air,in}$	^oC	M	284.2	285.3	284.9	294.6
$T_{air,out}$	^oC	C	323.2	357.9	391.6	430.9
$\dot{m}_{air}$	kg/s	C	1.96	2.65	3.5	4.27
β_{comp}	-	M				
Turbine						
$T_{eg,in}$	^oC	M	729.5	762.1	770.3	798.5
$T_{eg,out}$	^oC	M	652.8	667.8	654.2	659.4
$\dot{m}_{eg}$	kg/s	C	2.02	2.74	3.61	4.41
β_{exp}	-	C				
Cylinders						
$\dot{m}_{air,in}$	kg/s	C	1.96	2.65	3.5	4.27
$\dot{m}_{fuel,in}$	kg/s	C	0.05	0.08	0.11	0.14
$\dot{m}_{eg,out}$	kg/s	C	2.02	2.74	3.61	4.41
$T_{air,in}$	^oC	M	320.8	322.3	327.6	329.1
$T_{eg,out}$	^oC	C	729.5	762.1	770.3	798.5
CAC-LT stage						
$T_{air,in}$	^oC	C	323.2	356.3	366.7	372.0
$T_{air,out}$	^oC	M	320.8	322.3	327.6	329.1
$T_{w,in}$	^oC	M	317.1	316.3	317.5	314.1
$T_{w,out}$	^oC	C	317.2	318.2	320.5	318.3
$\dot{m}_{w,LT}$	kg/s	C	11.16	11.16	10.98	10.78
CAC-HT stage						
$T_{air,in}$	^oC	C	323.2	357.9	391.6	430.9
$T_{air,out}$	^oC	C	323.2	356.3	366.7	372.0
$T_{w,in}$	^oC	C	362.5	364.2	368.0	368.2
$T_{w,out}$	^oC	C	362.5	364.3	369.3	371.9
$\dot{m}_{w,HT}$	kg/s	C	16.66	16.67	16.55	16.67
LOC						
$T_{lo,in}$	^oC	C	348.2	350.3	354.0	357.3
$T_{lo,out}$	^oC	M	336.6	337.4	339.7	340.4
$T_{w,in}$	^oC	C	317.2	318.2	320.5	318.3
$T_{w,out}$	^oC	C	325.9	327.8	331.4	331.3
JWC						
T_{wall}	^oC	C		4	23	
$T_{w,in}$	^oC	M	360.0	359.7	362.3	361.5
$T_{w,out}$	^oC	C	362.5	364.2	368.0	368.2

Table 2: Auxiliary engines, measured and calculated temperatures and flows at different engine loads

Energy flow	type	30%	50%	70%	90%
Power output	Mech	1767	2946	4118	5293
Exhaust gas (after turbine)	Heat	1672	2566	3227	3938
CAC-LT	Heat	104	152	279	454
CAC-HT	Heat	2	337	569	843
JWC	Heat	381	249	278	318
LOC	Heat	682	721	699	725

Table 3: Main engines, energy flows at different engine loads

Energy flow	type	30%	50%	70%	90%
Power output	Mech	828	1381	1932	2482
Exhaust gas (after turbine)	Heat	808	1144	1456	1753
CAC-LT	Heat	5	91	139	216
CAC-HT	Heat	0	5	89	257
JWC	Heat	176	314	396	467
LOC	Heat	405	448	499	587

Table 4: Auxiliary engines, energy flows at different engine loads

A representation of the ship cooling systems is provided in Figure XXX.

All values not directly measured in the cooling systems were calculated based on mass and energy balances.

Figure cooling systems

2.5. Estimation of the electric power demand

The total electric power demand of the system is easily estimated as the sum of the power generated by the four auxiliary engines, that is directly measured on the electrical side of the generators and has a rather high accuracy

$$P_{el,tot} = \sum_{1}^{4} AE_i \tag{12}$$

The determination of how different consumers contribute to the total electric power demand is less trivial. The ship is equipped with a number of different systems, including lighting, navigational systems, pumps and compressors, etc. None of the individual contributions is directly measured, hence estimations need to be based on indirect measurements.
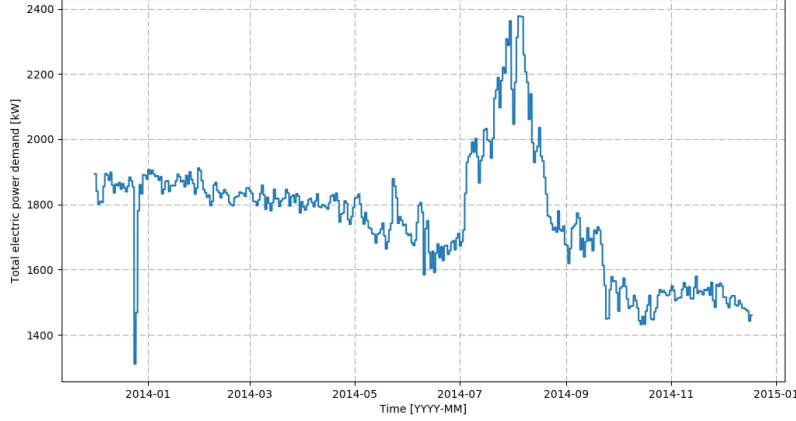
Figure 4: Total electric power demand versus time (Daily average)

2.5.1. HVAC systems

For what concerns the air conditioning unit demand (HVAC), the observation of the total power demand over the year (see Figure 4, showing daily averages) leads to the identification of a clear period, corresponding to the summer months, during which there is a significant increase of the demand.

Since the total demand seems to be rather constant otherwise, it can be concluded that the demand of the HVAC compressors related to the need for cooling is concentrated during the summer months. Additionally, comparing the evolution of the daily demand (see Figure 5, representing the instantaneous demand divided by the daily average) between a random summer and winter day, shows that the daily variation is comparable. This shows that assuming a constant consumption for the HVAC during the day does not introduce a substantial error in the estimations.

Hence, the HVAC electric power demand was estimated as follows:

$$P_{el,HVAC} = \begin{cases} P_{el,tot}(t) - P_{el,ref}(t), & \text{if } 2014\text{-}07\text{-}03 < t < 2014\text{-}08\text{-}21 \\ 0, & \text{otherwise} \end{cases} \tag{13}$$

where $P_{el,ref}(t)$ is calculated as:

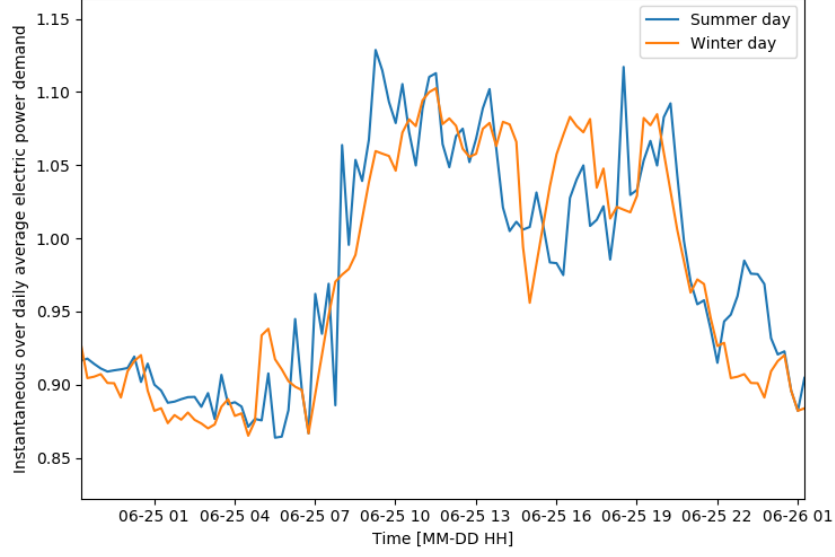$$P_{el,ref}(t) = 0.5(P_{el,tot}(t_1) + P_{el,tot}(t_2)) \tag{14}$$

16

Figure 5: Instantaneous power demand over daily average, winter versus summer day

2.5.2. Thrusters

When entering port areas, the ship needs to use thrusters to maneuver and berth. In the case of this particular ships, operating on daily schedules and hence maneuvering four times per day, the power demand related to thrusters can be significant. In order to isolate the demand from the thrusters, we created a reference daily energy profile, based on the instantaneous electric power demand divided by the daily average. From this daily profile (made of 96 points), we selected manually selected the points that could be clearly identified as related to the thrusters energy demand, and substituted the actual value with a weighted average of the previous and subsequent points (see Figure 6).

By comparing the reference profile to the instantaneous one, the points where the former is more than 10% higher than the latter are identified as "thruster-on" points and treated consequently.

2.6. Estimation of the heat demand

As the heat demand is not measured, it is necessary to determine it based on the available indirect measurements.
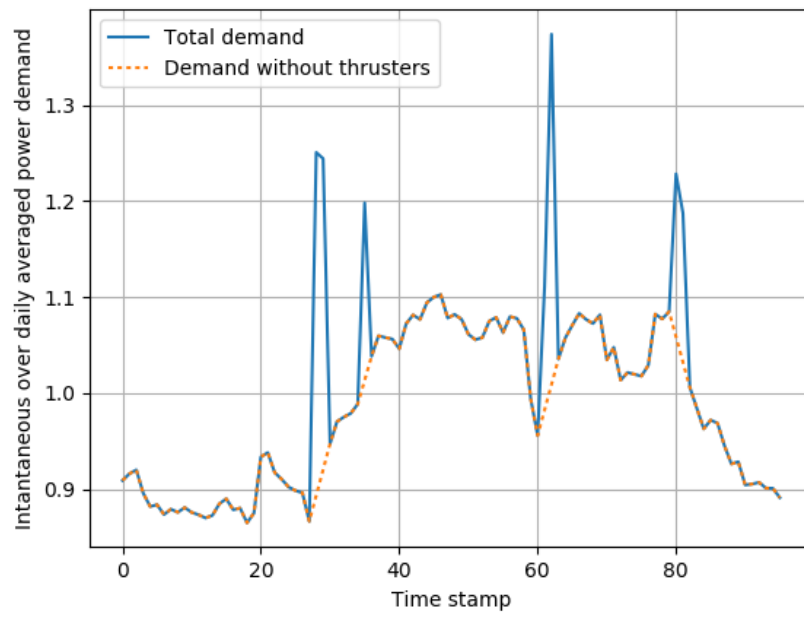
17

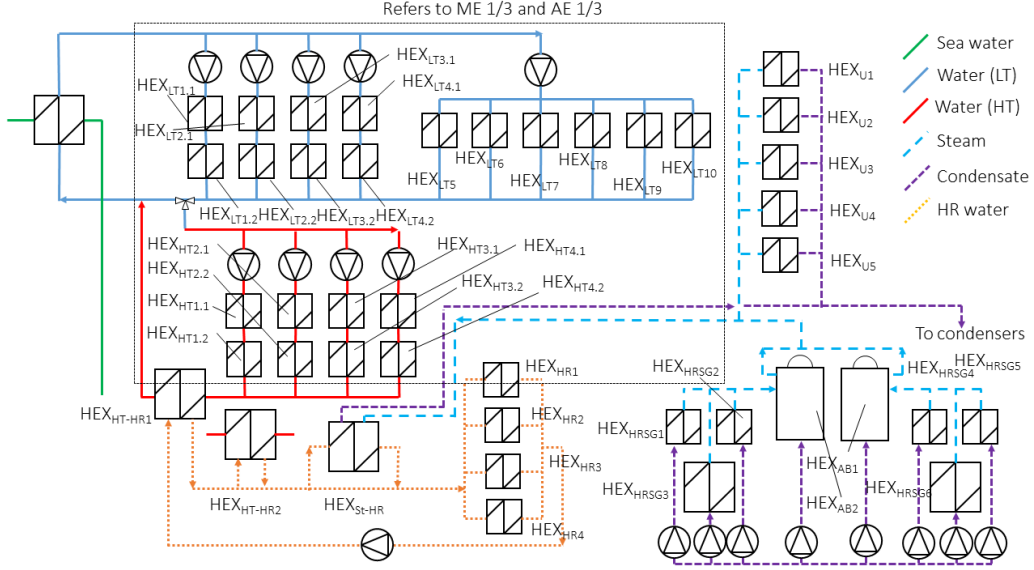Figure 6: Example of the procedure of selection of thruster power demand

Figure 7: General view of the ship heating and cooling systems

The heat demand and generation can be summarized according to the following equations:

$$\dot{Q}_{gen} = \dot{Q}_{EGB} + \dot{Q}_{HTHR} + \dot{Q}_{AB} \tag{15}$$
$$\dot{Q}_{dem} = \dot{Q}_{HVAC,PH} + \dot{Q}_{HVAC,RH} + \dot{Q}_{HWH} + \dot{Q}_{TH} + \dot{Q}_G + \dot{Q}_{OT} + \dot{Q}_{HTH} + \dot{Q}_{MSH} \tag{16}$$
$$\tag{17}$$

The main view of the ship heating and cooling systems is presented in Figure 7

2.6.1. Heat balance parameter estimation

As not enough information and measurements are available to determine the various components of the heat balance, in this paper we determined them by means of a parameter estimation procedure, using the daily boiler fuel consumption for the calibration of the parameters. The parameter estimation problem is hence written as a minimization problem:

$$min \quad \left(\frac{\sum_i (y(\mathbf{p}) - \bar{y})^2}{\sum_i \bar{y}^2} \right)^{0.5} \tag{18}$$

$$\tag{19}$$

where the vector **p** includes the calibration parameters that are part of the heat demand and generation estimation model that is explained in detail in the following sections. A list of the parameters **p** is shown in Table REF, together with the chosen upper and lower boundaries for the calibration procedure.

2.6.2. Heat demand

We calculated the heat demand as the sum of the contributions of the elements listed in the ship's heat balance documentation. As no direct measurement of these quantities was available in the dataset, they had to be estimated based on the following assumptions:

where all f_i factors are treated as calibration parameters (see table 5). The $\Phi_G(\hat{t})$ and $\Phi_{HWH}(\hat{t})$ functions represent the assumption made on the daily evolution of the heating demand from the galley and the hot water heater respectively. The daily evolutions of the demand are considered to be the same over the whole year of operations and are represented graphically in Figure REF.

2.6.3. Heat generation

The heat recovered in the EGBs is the only contribution to the heat balance that is known with a reasonable certainty. The heat transferred from the exhaust gas to the steam ($\dot{Q}_{EGB}$) is calculated according to equation 2.6.3:

$$\dot{Q}_{EGB} = \dot{m}_{eg}c_{p,eg}(T_{eg,EGB,in} - T_{eg,EGB,out}) \qquad (20)$$

where $T_{eg,EGB,out}$ and $T_{eg,EGB,in}$ are measured for all EGBs, $c_{p,eg}$ is calculated as a function of the exhaust gas composition and temperature, and $\dot{m}_{eg}$ is calculated based on the engine energy and mass balance as described in section REF and in the appendix REF

It is known that the ship heating systems are designed for recovering energy from the high temperature cooling systems of all the ship's engines. However, measurements of this contribution and of other variables that could lead to its straight-forward identification are missing. In this work, we calculated the heat exchanged in the two HTHRs according to equation ,

Parameter name	Symbol	Unit	Lower Boundary	Higher Boundary	Optimal value
Constant HTHR heat demand	$\dot{Q}_{k,HTHR}$	kW	0	1000	
Constant steam demand	$\dot{Q}_{k,steam}$	kW	0	1000	
Weight factor of the HVAC Reheater	$f_{HVAC,RH}$	-	0.5	1	
Weight factor of the HVAC Preheater	$f_{HVAC,PH}$	-	0	1	
Weight factor of hot water heater	f_{HWH}	-	0.5	1	
Weight factor of the galley	f_G	-	0.5	1	
Weight factor of the other consumers	f_{Other}	-	0.5	1	
HTHR inlet temperature	$T_{HTHR,ER1,in}$	K	343	353	
Effectiveness of the HTHR HEX	ϵ_{HTHR}	-	0.5	0.9	
Boiler drum steam storage capacity	$Q_{ab,max}$	MJ	100	100000	
Boiler heat rate	$\dot{Q}_{ab,des}$	kW	2000	8000	

Table 5: Parameters optimized in the parameter estimation for the heat balance

Heat flow name	Equation
HVAC Pre-heater	$\dot{Q}_{HVAC,PH} = f_{HVAC,RH}\dot{Q}_{HVAC,PH,des}\dfrac{\dot{W}_{HVAC}(t)}{\dot{W}_{HVAC,max}}$
HVAC Re-heater	$\dot{Q}_{HVAC,RH} = f_{HVAC,PH}\dot{Q}_{HVAC,PH,des}\dfrac{T_{in} - T_{air,out}(t)}{T_{in} - T_{air,out,des}}$
Hot water heater	$\dot{Q}_{HWH} = f_{HWH}\dot{Q}_{HWH,des}\Phi_{HWH}(\hat{t})$
Galley	$\dot{Q}_G = f_G\dot{Q}_{G,des}\Phi_G(\hat{t})$
Low temperature tank heating	$\dot{Q}_{TH} = f_{TH}\dot{Q}_{TH}\dfrac{T_T - T_{air,out}(t)}{T_T - T_{air,out,des}}$
HFO tank heating	$\dot{Q}_{HTH} = f_{HTH}\dot{Q}_{HTH}\dfrac{T_{HT} - T_{air,out}(t)}{T_{HT} - T_{air,out,des}}$
Machinery space heating	$\dot{Q}_{MSH} = f_{MSH}\dot{Q}_{MSH}\dfrac{T_{MS} - T_{air,out}(t)}{T_{MS} - T_{air,out,des}}$
HFO heater	$\dot{Q}_{HH} = \dot{m}_{HFO}(t)c_{p,HFO}(T_{HFO,inj} - T_{HT})$

Table 6: Summary of the heat demand contributions and their calculation

$$\dot{Q}_{HTHR} \quad = \quad \dot{Q}_{HTHR,ER1} + \dot{Q}_{HTHR,ER2} \tag{21}$$

$$= \sum_{i=ER1,ER2} \epsilon_{HTHR} * \dot{m}_{min,HTHR,i} * c_{p,w} * (T_{HT,out,i} - T_{HRHT,i,in}) \tag{22}$$

where the effectiveness of the heat exchanger ϵ_{HTHR} is considered to be constant and its value is part of the parameter estimation problem (see table 5). The HT water outlet temperature for each engine room is calculated based on the thermal balance of the engines, and the HR water at the HTHR inlet ($T_{HRHT,ER1,in}$) is considered as a calibration parameter.

The heat generated by the auxiliary boilers is calculated as to close the heat balance of the ship energy systems. The contribution of the boiler heat storage capacity is taken into account by a calibration parameter $Q_{ab,max}$ that determines the maximum heat deficit. This corresponds, in practice, to assuming that the boiler is started up when the steam pressure inside the boiler drops below a certain value, and stopped once the pressure has achieved its maximum operative value. In this calculation, the calibration parameters are the heat storage capacity ($Q_{ab,max}$) and the fixed heat rate ($\dot{Q}_{ab,des}$) of the auxiliary boilers (see table 5).

2.6.4. Parameter estimation and uncertainty quantification

The results of the parameter estimation are represented graphically and quantitatively in Figure REF and Table REF.

Given the lack of input values for the estimation of the heat demand, the provided estimate based on the procedure described above should be integrated with an estimation of the uncertainty.

In this study, we base the estimation of the uncertainty on the production side, as it is the one that has the largest amount of information available. In these regards, the uncertainty can be reduced to the contribution of three elements: $U(\dot{Q}_{EGB})$, $U(\dot{Q}_{HTHR})$, $U(\dot{Q}_{AB})$.

The uncertainty on the heat generated in the EGBs can be further subdivided based on its definition as a composition of the uncertainty of $T_{eg,EGB,in}$, $T_{eg,EGB,out}$, $\dot{m}_{eg}$, and $c_{p,eg}$. In the case of $T_{eg,EGB,in}$ and $T_{eg,EGB,out}$, measured values are used, where the uncertainty is related to the sensors (K-type thermocouples) that can be as high as 4% [CIT]. The uncertainty on the $\dot{m}_{eg}$ is related to the calculation assumptions as described in Appendix REF, and can be estimated of being up to 10%. The uncertainty of the $c_{p,eg}$ value,

given that both composition and temperature are accounted for, should be within 5% of the reference value. These assumptions lead to the following estimation of the uncertainty:

$$\frac{\delta \dot{Q}_{gen}}{\dot{Q}_{gen}} = \sqrt{\frac{\delta \dot{m}_{eg}^2}{\dot{m}_{eg}^2} + \frac{\delta c_{p,eg}^2}{c_{p,eg}^2} + \frac{\delta T_{EGB,in}^2 + \delta T_{EGB,out}^2}{(T_{EGB,in} - T_{EGB,out})^2}} \qquad (23)$$

That once typical values are assigned can be as high as 30%, where most of the variability is related to the temperature measurements (result obtained for ±20 K uncertainty. The uncertainty is reduced to 20% if the measurement uncertainty on the temperature is reduced to ±20 K)

The uncertainty of the heat generated by the ABs can be reduced to the contribution of two elements: the uncertainty on $\dot{m}_{fuel,AB}$ and that on η_{AB}. The former will be at least as large as the calibration error (35%) and will be considered equal to 50% to be conservative and accounting also for errors in the aggregated boiler fuel measurements. In addition, the uncertainty on the efficiency can be considered to be around 10% based on the discrepancy between the considered sources and on the expected variability of the efficiency with load. Similarly to the previous case, the combination of these efficiencies lead to a total uncertainty of 51%, where the main contribution comes from the uncertainty of the model output compared to the actual fuel consumption.

The estimation of the uncertainty of $\dot{Q}_{HTHR}$ can be based on 22 having assigned an acceptable variation of 20% to the effectiveness of the heat exchanger, 20% on the estimation of the reference mass flow, ±5 K uncertainty on water temperature measurements and considering negligible the uncertainty on $c_{p,w}$, leading to a 145% uncertainty on this measurement.

2.7. Determination of typical operational days

3. Results (and discussion)

3.1. Exploratory analysis

In this section, we observe and analyze direct measurements from ship systems, with no pre-processing, that are expected to have an influence on the energy analysis.

Figures 8a and 8b represent the time evolution and the distribution over the year of the ambient air and sea water temperature. The relatively low

temperatures that are experienced by the case study ship during its operations suggest that heating demand can be expected to be higher than cooling demand. On the other hand, the fact that, in summer, air temperatures reach up to 26 degrees Celsius justify the existence of an HVAC unit that can also operate in cooling mode.
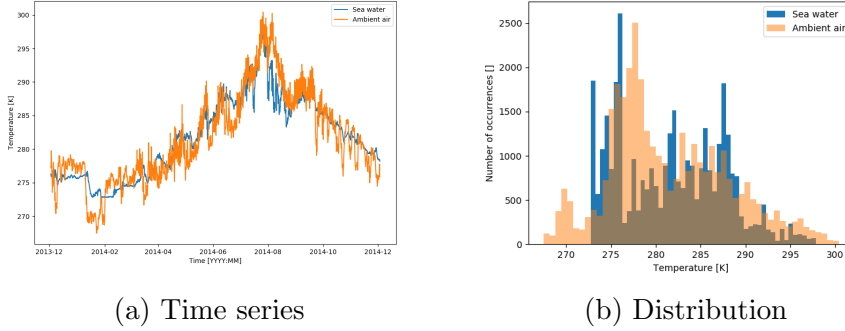

(a) Time series   (b) Distribution

Figure 8: Statistical representation of measured air and sea water temperatures based on yearly data. Landsort, 2014

Figure 9 represents the distribution of the ship speed, both in terms of statistical distribution and in terms of a reference 24h period. The ship operates almost for the entire year according to a fix schedule, while there are a couple of periods (particularly during the summer months) when the ship operates at higher speed. This can also be seen from Figure **??**, where the main cluster of operations at middle-low speed can be clearly identified, as well as the smaller area of operations at high speed.

figure –¿ Operational mode distribution

ANYTHING ELSE THAT CAN BE INTERESTING TO SHOW IN THE EXPLORATORY DATA ANALYSIS?

3.2. Energy analysis

Here we can see the typical example (note: the day was not selected as "typical", but simply randomly) of the energy demand during a winter and a summer day (Figures 12 and 13). It can be seen clearly how, as expected, the heating demand in winter is much higher than in summer [2800-4500 kW vs 1100-2900 kW], as a consequence of the reduce need for compartment heating. On the other hand, the electric power demand behaves inversely, ranging around 1900 kW during the reference winter day (peaks are connected to
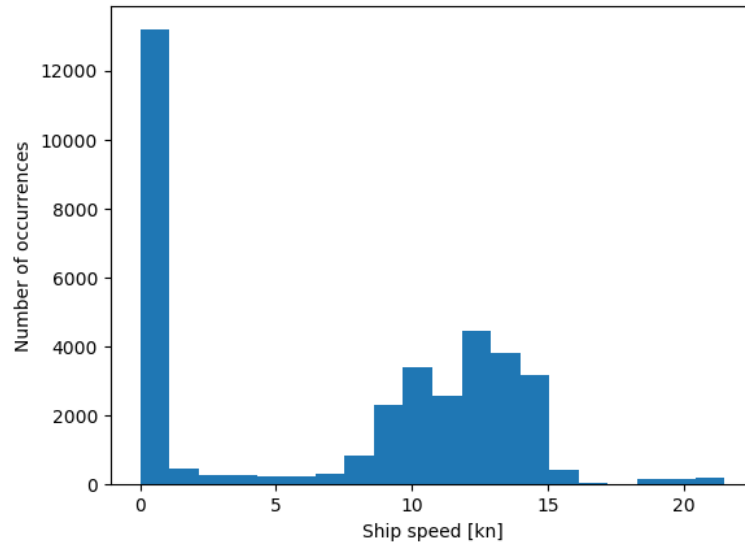
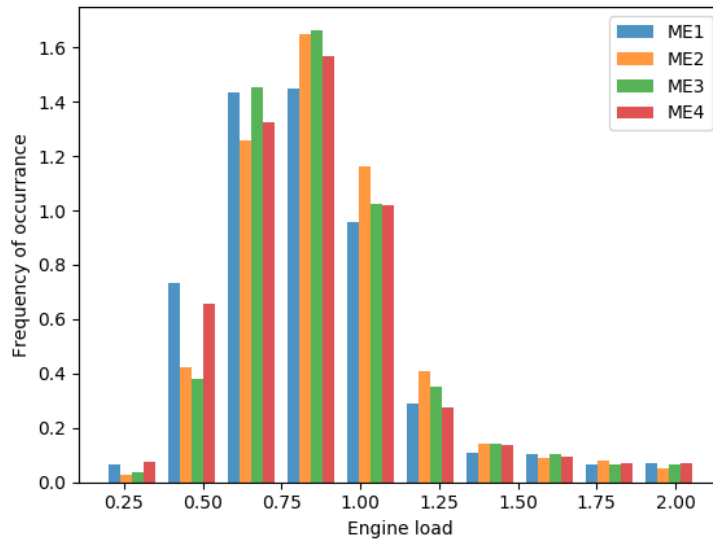Figure 9: Yearly distribution of ship speed

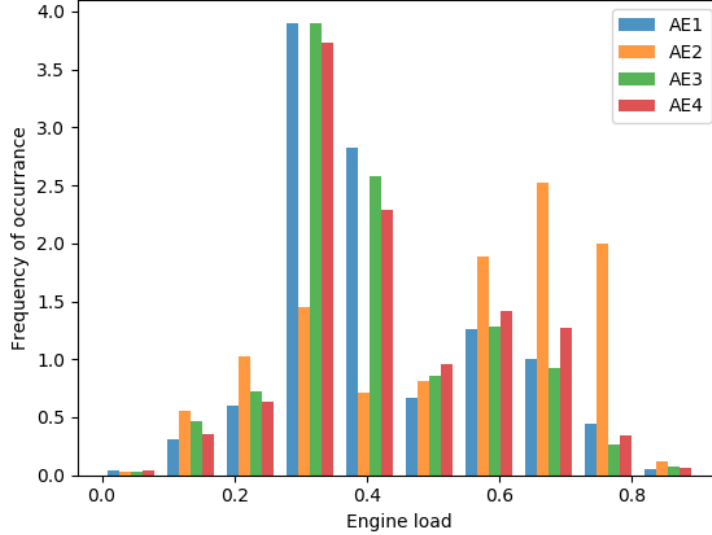Figure 10: Yearly load distribution, main engines

Figure 11: Yearly load distribution, auxiliary engines

the use of thrusters in port for maneuvering) and around 2300 kW during the reference summer day, where the difference is mostly associated to the demand of the HVAC compressors.

From Figure 14 it can be noted that nearly 50% of the total energy demand is related to ship propulsion, while the remaining portion is approximately equally split between electric energy and heat demand.

Within the electric energy demand, the HVAC systems only represent a minor contribution (XX%), as it is only present for a few months during summer, and at rather low power demand. This is not surprising, since it can be observed that (see Figure 8b) the air is always below 27°C, and rarely above 17°C. Also the thrusters, although they represent a rather high instantaneous demand, they are only used for a very short time and, hence, their total contribution to the ship energy demand is limited to XX%. As a consequence, most of the electric energy demand should be allocated to other consumers, and efforts should be directed towards providing additional measurements of how different users contribute to the total electric power demand.
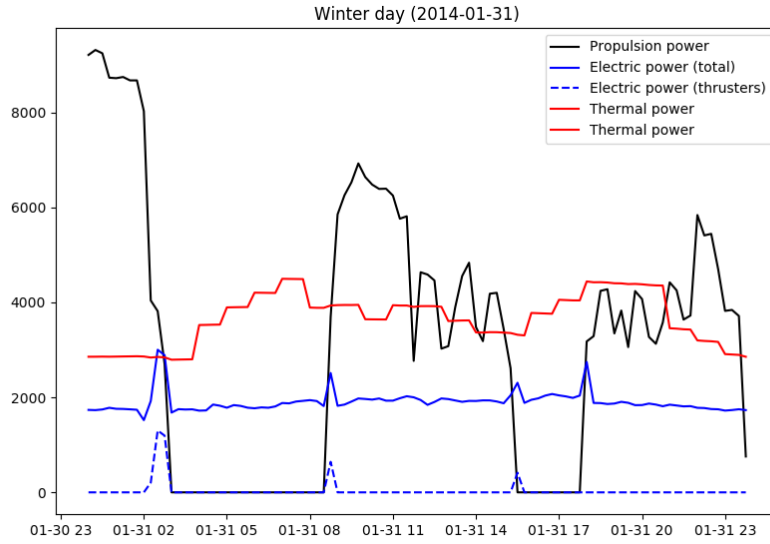
Figure 12: Energy demand during a day of operations, Winter
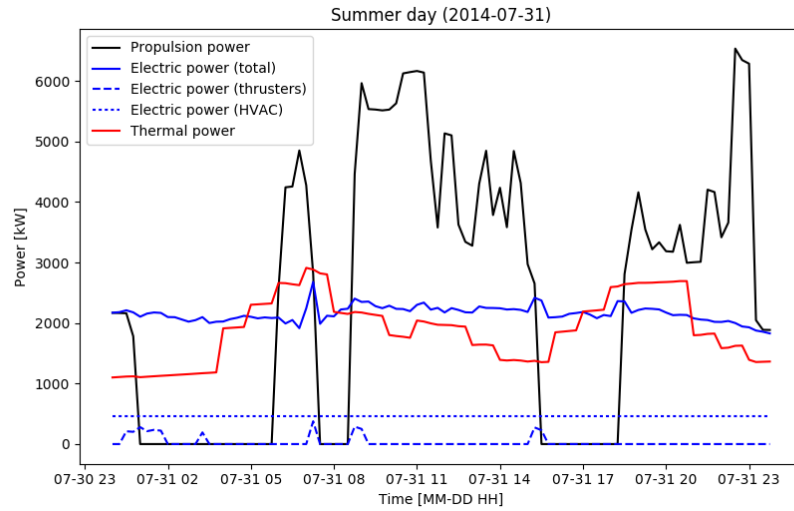

Figure 13: Energy demand during a day of operations, Summer
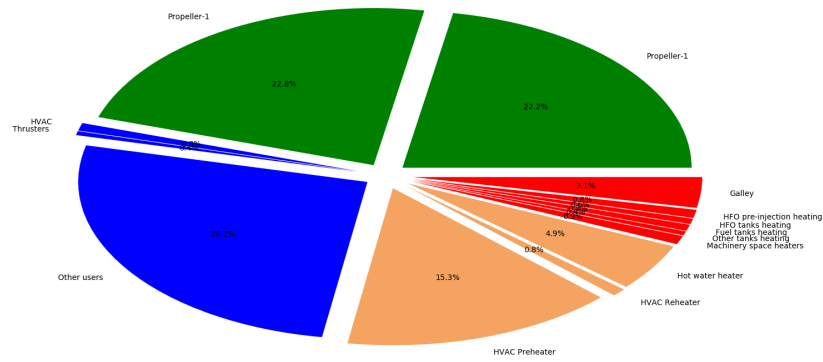
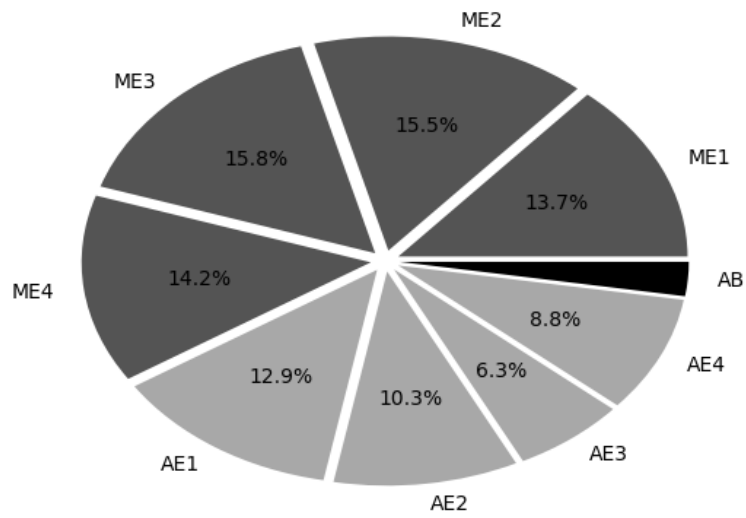Figure 14: Energy demand, aggregated data for one year of operations

Figure 15: Energy generation, aggregated data for one year of operations
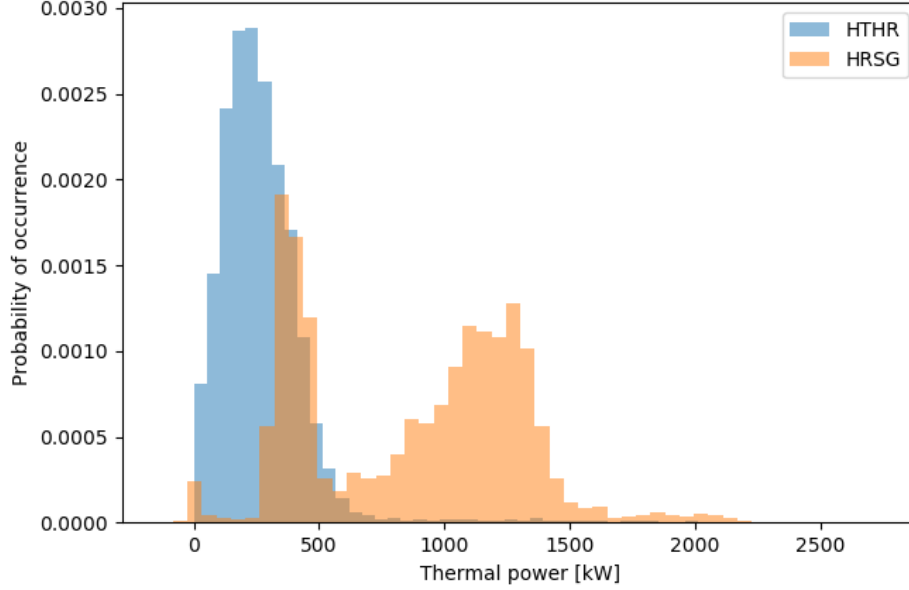
Figure 16: Distribution of thermal power generated from on board waste heat recovery

3.3. Heat demand and generation

FIGURE –¿ Pie, heat generated by source FIGURE –¿ filled lines, heat generated by source.

Looking at Figure **??** it is possible to appreciate the amount of heat that is recovered from on board available waste heat (cooling water and exhaust gas). It can be observed that the amount of heat recovered from the HT cooling systems is much lower than expected, with an average of around 350 kW. This value is quite unreasonable compared to the values found in the technical specifications from the yard, that go from 700 kW (when only one auxiliary engine is operated) to 4800 kW (when all main engines and two auxiliary engines are operated).

Regarding the heat demand onboard, it can be seen that the HVAC reheater represents the largest contributor (XX%) followed by the hot water heater (XX%). The large contribution of the HVAC reheater can be explained by the former being important for long times and in relation to the low ambient temperatures encountered by the case study vessel during oper-

ation. The relatively large contribution of the hot water heater can instead be related to the fact that these systems are rather important consumers and are necessary during the whole ship operations (i.e. also during the summer months).

3.4. Exergy Analysis

The results of the exergy analysis of the ship energy systems are shown in Figure REF and Tables REF to REF.

Table(s) –¿ Exergy efficiencies - General at system level - One per system (MEs, AEs, CoolingSystems, SteamSystems)

Figure –¿ Grassman diagram

3.5. Typical operational days

4. Conclusion

Appendix A. Full tables of energy and exergy flows

Appendix B. Full equation list

Before compressor	$T_{comp,in} = \text{Measured}$ $p_{comp,in} = \text{Measured}$
After compressor	$T_{comp,out} = T_{comp,in} + \frac{T_{comp,out,is} - T_{comp,in}}{\eta_{comp,is}}$ $p_{comp,out} = \text{Measured}$ $\eta_{comp,is} = P_2\left(\frac{p_{comp,out}}{p_{comp,in}}\right)$
After CAC-HT stage	$p_{CAC-HT,out} = p_{comp,out}$ $T_{CAC-HT,out} = T_{comp,out} - \frac{\dot{Q}_{CAC,HT}}{\dot{m}_{air,cyl}}$ $\dot{Q}_{CAC,HT} = P_2(\lambda)$
After CAC-LT stage	$p_{CAC-LT,out} = p_{comp,out}$ $T_{CAC-LT,out} = T_{CAC-HT,out} - \frac{\dot{Q}_{CAC,LT}}{\dot{m}_{air,cyl}}$ $\dot{Q}_{CAC,LT} = P_2(\lambda)$
After CAC-LT stage	

Appendix C. Estimation of air and exhaust gas flows in the main engines

Appendix C.1. Mass balances

Mass balance on the split after the compressor, with one flow going to the engine inlet valves and the other flow going to the bypass valve

$$\dot{m}_{air,comp} = \dot{m}_{air,cyl} + \dot{m}_{air,bypass} \tag{C.1}$$

Mass balance on the mixer before the turbine, with one flow coming from the engine exhaust valves and the other flow coming from the bypass valve

$$\dot{m}_{eg,turb} = \dot{m}_{eg,cyl} + \dot{m}_{air,bypass} \tag{C.2}$$

Note that the exhaust gas mass flow from the cylinders is fully defined as follows:

$$\dot{m}_{eg,cyl} = \dot{m}_{air,cyl} + \dot{m}_{fuel,cyl} \tag{C.3}$$

Appendix C.2. Energy balances

Energy balance on the turbocharger: the power generated by the turbine must be equal to the power absorbed by the compressor

$$\dot{m}_{air,comp}\Delta h_{comp} = \dot{m}_{eg,turb}c_{p,eg}(T_{turb,in} - T_{turb,out})\eta_{mech} \tag{C.4}$$

Energy balance on the mixer between the air flow after the bypass valve and the exhaust gas flow after the exhaust valve

$$\dot{m}_{air,bypass}c_{p,air}(T_{comp,out}-T_0)+\dot{m}_{eg,cyl}c_{p,eg}(T_{cyl,out}-T_0) = \dot{m}_{eg,turb}c_{p,eg}(T_{turb,in}-T_0) \tag{C.5}$$

The system of four equations is to be solved in the four following unknowns:

- $\dot{m}_{eg,turb}$

- $\dot{m}_{air,bypass}$

- $\dot{m}_{air,comp}$

- $T_{turb,in}$ (In the case of the Main engines)

- $T_{cyl,out}$ (In the case of the Auxiliary engines)

Include other assumptions: - TC efficiency - Compressor efficiency - Turbine efficiency

Appendix C.3. Main Engines

To calculate what we need, we must make the system explicit on the variables we need to calculate. This process is different for the main and auxiliary engines, mostly because the temperature measurement of the exhaust gas before the turbine is positioned differently. In the case of the main engines, the temperature at the **cylinder outlet** is measured and, hence, known.

First, we make all equations explicit in $\dot{m}_{air,bypass}$ thus eliminating both $\dot{m}_{eg,turb}$ and $\dot{m}_{air,comp}$

$$(\dot{m}_{air,cyl}+\dot{m}_{air,bypass})\Delta h_{comp} = (\dot{m}_{eg,cyl}+\dot{m}_{air,bypass})c_{p,eg}(T_{turb,in}-T_{turb,out})\eta_{mech}$$

$$\dot{m}_{air,bypass}c_{p,air}(T_{comp,out}-T_0)+\dot{m}_{eg,cyl}c_{p,eg}(T_{cyl,out}-T_0) = (\dot{m}_{eg,cyl}+\dot{m}_{air,bypass})c_{p,eg}(T_{turb,in}-T_0)$$

At this point, we use the first equation to simplify the system and make it explicit in the $\dot{m}_{air,bypass}$ variable alone:

$$
\begin{aligned}
(\dot{m}_{eg,cyl} + \dot{m}_{air,bypass})c_{p,eg}(T_{turb,in} - T_{turb,out})\eta_{mech} &= (\dot{m}_{air,cyl} + \dot{m}_{air,bypass})\Delta h_{comp} \\
T_{turb,in} - T_{turb,out} &= \frac{\dot{m}_{air,cyl} + \dot{m}_{air,bypass}}{\dot{m}_{eg,cyl} + \dot{m}_{air,bypass}} \frac{\Delta h_{comp}}{c_{p,eg}\eta_{mech}} \\
T_{turb,in} &= T_{turb,out} + \frac{\dot{m}_{air,cyl} + \dot{m}_{air,bypass}}{\dot{m}_{eg,cyl} + \dot{m}_{air,bypass}} \frac{\Delta h_{comp}}{c_{p,eg}\eta_{mech}}
\end{aligned}
$$

We can now substitute this expression in the second equation:

$$\dot{m}_{air,bypass}c_{p,air}(T_{comp,out} - T_0) + \dot{m}_{eg,cyl}c_{p,eg}(T_{cyl,out} - T_0) =$$
$$(\dot{m}_{eg,cyl} + \dot{m}_{air,bypass})c_{p,eg}(T_{turb,out} + \frac{\dot{m}_{air,cyl} + \dot{m}_{air,bypass}}{\dot{m}_{eg,cyl} + \dot{m}_{air,bypass}} \frac{\Delta h_{comp}}{c_{p,eg}\eta_{mech}} - T_0)$$

$$(C.6)$$

We first execute the multiplication in the term on the right of the equal:

$$\dot{m}_{air,bypass}c_{p,air}(T_{comp,out} - T_0) + \dot{m}_{eg,cyl}c_{p,eg}(T_{cyl,out} - T_0) =$$
$$\dot{m}_{eg,cyl}c_{p,eg}(T_{turb,out} - T_0)+$$
$$\dot{m}_{air,bypass}c_{p,eg}(T_{turb,out} - T_0)+$$
$$\frac{\Delta h_{comp}}{c_{p,eg}\eta_{mech}}(\dot{m}_{air,cyl} + \dot{m}_{air,bypass})c_{p,eg} \quad (C.7)$$

Now, we can group together the elements in the variable of interest:

$$\dot{m}_{air,bypass}\left[c_{p,air}(T_{comp,out} - T_0) - c_{p,eg}(T_{turb,out} - T_0) - \frac{\Delta h_{comp}}{\eta_{mech}}\right] =$$
$$\dot{m}_{eg,cyl}c_{p,eg}(T_{turb,out} - T_0) - \dot{m}_{eg,cyl}c_{p,eg}(T_{cyl,out} - T_0) + \frac{\Delta h_{comp}}{\eta_{mech}}\dot{m}_{air,cyl} \quad (C.8)$$

This can be further simplified into:

$$\dot{m}_{air,bypass}\left[c_{p,air}(T_{comp,out} - T_0) - c_{p,eg}(T_{turb,out} - T_0) - \frac{\Delta h_{comp}}{\eta_{mech}}\right] =$$
$$\dot{m}_{eg,cyl}c_{p,eg}(T_{turb,out} - T_{cyl,out}) + \frac{\Delta h_{comp}}{\eta_{mech}}\dot{m}_{air,cyl} \quad (C.9)$$

Finally, we can assume the specific heat at constant pressure of air and exhaust gas to be sufficiently similar for considering them equal in the term at the numerator (we ignored changes in the properties of the mixture in other points as well):

$$\dot{m}_{air,bypass}\left[c_{p,eg}(T_{comp,out} - T_{turb,out}) - \frac{\Delta h_{comp}}{\eta_{mech}}\right] =$$
$$\dot{m}_{eg,cyl}c_{p,eg}(T_{turb,out} - T_{cyl,out}) + \frac{\Delta h_{comp}}{\eta_{mech}}\dot{m}_{air,cyl} \quad (C.10)$$

From which we can derive the final form:

$$\dot{m}_{air,bypass} = \frac{\dot{m}_{eg,cyl}c_{p,eg}(T_{turb,out} - T_{cyl,out}) + \frac{\Delta h_{comp}}{\eta_{mech}}\dot{m}_{air,cyl}}{c_{p,eg}(T_{comp,out} - T_{turb,out}) - \frac{\Delta h_{comp}}{\eta_{mech}}} \quad (C.11)$$

Which can be rewritten, in order to have both numerator and denominator positive, as follows:

$$\dot{m}_{air,bypass} = \frac{\dot{m}_{eg,cyl}c_{p,eg}(T_{cyl,out} - T_{turb,out}) - \frac{\Delta h_{comp}}{\eta_{mech}}\dot{m}_{air,cyl}}{c_{p,eg}(T_{turb,out} - T_{comp,out}) - \frac{\Delta h_{comp}}{\eta_{mech}}} \quad (C.12)$$

Appendix C.4. Auxiliary Engines

In the case of the auxiliary engines, what we know instead is the temperature of the exhaust gas **before the turbine**, hence after the merging between the exhaust gas and the bypass.

In this case, however, things appear to be simple: the energy balance on the turbocharger can be calculated as there is only one variable unknown: the total mass flow in the compressor, and hence the bypass flow:

$$(\dot{m}_{air,cyl}+\dot{m}_{air,bypass})\Delta h_{comp} = (\dot{m}_{eg,cyl}+\dot{m}_{air,bypass})c_{p,eg}(T_{turb,in}-T_{turb,out})\eta_{mech}$$

$$\dot{m}_{air,cyl}\Delta h_{comp}+\dot{m}_{air,bypass}\Delta h_{comp} = \dot{m}_{eg,cyl}c_{p,eg}(T_{turb,in}-T_{turb,out})+\dot{m}_{air,bypass}c_{p,eg}(T_{turb,in}-T_{turb,out})\eta_m$$

$$\dot{m}_{air,bypass}(\Delta h_{comp}-c_{p,eg}(T_{turb,in}-T_{turb,out})\eta_{mech}) = \dot{m}_{eg,cyl}c_{p,eg}(T_{turb,in}-T_{turb,out})-\dot{m}_{air,cyl}\Delta h_{comp}$$

$$\dot{m}_{air,bypass} = \frac{\dot{m}_{eg,cyl}c_{p,eg}(T_{turb,in}-T_{turb,out})\eta_{mech}-\dot{m}_{air,cyl}\Delta h_{comp}}{\Delta h_{comp}-c_{p,eg}(T_{turb,in}-T_{turb,out})\eta_{mech}} \quad (C.13)$$

Now that we have the value for the bypass flow, it is easy to calculate backwards the temperature of the exhaust gas after the cylinder outlet valves, before the merging with the bypass flow:

$$\dot{m}_{air,bypass}c_{p,air}(T_{comp,out}-T_0)+\dot{m}_{eg,cyl}c_{p,eg}(T_{cyl,out}-T_0) = \dot{m}_{eg,turb}c_{p,eg}(T_{turb,in}-T_0)$$

$$\dot{m}_{eg,cyl}c_{p,eg}(T_{cyl,out}-T_0) = \dot{m}_{eg,turb}c_{p,eg}(T_{turb,in}-T_0)-\dot{m}_{air,bypass}c_{p,air}(T_{comp,out}-T_0)$$

$$T_{cyl,out} = T_0 + \frac{\dot{m}_{eg,turb}c_{p,eg}(T_{turb,in}-T_0)-\dot{m}_{air,bypass}c_{p,air}(T_{comp,out}-T_0)}{\dot{m}_{eg,cyl}c_{p,eg}}$$
$$(C.14)$$

Appendix D. Full list of available measurements

References

[1] T.W.P. Smith, J. P. Jalkanen, B.A. Anderson, James J Corbett, J. Faber, Hanayama S., E. O'Keeffe, S. Parker, L. Johansson, L. Aldous, C. Raucci, M. Traut, S. Ettinger, D. S. Lee, S. Ng, A. Agrawal, James J Winebrake, M. Hoen, S. Chesworth, and A. Pandey. Third IMO GHG Study. Technical report, International Maritime Organization (IMO), London, UK, 2014.

[2] UNCTAD. Review of maritime transport. united conference on trade and development.

[3] Karin Andersson, Selma Brynolf, J Fredrik Lindgren, and Magda Wilewska-Bien. *Shipping and the Environment.* Springer, Berlin, Germany, 2016.

[4] Evert A Bouman, Elizabeth Lindstad, Agathe I Rialland, and Anders H Strømman. State-of-the-art technologies, measures, and potential for reducing ghg emissions from shipping–a review. *Transportation Research Part D: Transport and Environment*, 52:408–421, 2017.

[5] W. Shi, D. Stapersma, and H. T. Grimmelius. Analysis of energy conversion in ship propulsion system in off-design operation conditions. *WIT Transactions on Ecology and the Environment*, 121:449–460, 2009.

[6] Gerasimos Theotokatos and Vasileios Tzelepis. A computational study on the performance and emission parameters mapping of a ship propulsion system. *Proceedings of the Institution of Mechanical Engineers , Part M : Journal of Engineering for the Maritime Environment*, 229(1):58–76, 2015.

[7] F. Tillig, J. Ringsberg, W. Mao, and B. Ramne. A generic energy systems model for efficient ship design and operation. *Proceedings of the Institution of Mechanical Engineers, Part M: Journal of Engineering for the Maritime Environment*, 2016.

[8] G Thomas, D O'Doherty, D Sterling, and C Chin. Energy audit of fishing vessels. *Proceedings of the Institution of Mechanical Engineers, Part M: Journal of Engineering for the Maritime Environment*, 224(November 2009):87–101, 2010.

[9] Oihane C. Basurko, Gorka Gabi??a, and Zigor Uriondo. Energy performance of fishing vessels and potential savings. *Journal of Cleaner Production*, 54:30–40, 2013.

[10] Charlotte Banks, Osman Turan, Atilla Incecik, G. Theotokatos, Sila Izkan, Catherine Shewell, and Xiaoshuang Tian. Understanding Ship Operating Profiles with an Aim to Improve Energy Efficient Ship Operations. In *Proceedings of the Low Carbon Shipping Conference*, pages 1–11, 2013.

[11] a. Coraddu, M. Figari, and S. Savio. Numerical investigation on ship energy efficiency by Monte Carlo simulation. *Proceedings of the Institution of Mechanical Engineers, Part M: Journal of Engineering for the Maritime Environment*, 228(3):220–234, 2014.

[12] Francesco Baldi, Gerasimos Theotokatos, and Karin Andersson. Development of a combined mean value-zero dimensional model and application for a large marine four-stroke Diesel engine simulation. *Applied Energy*, 154:402–415, 2015.

[13] Francesco Baldi and Cecilia Gabrielii. A feasibility analysis of waste heat recovery systems for marine applications. *Energy*, 80:654–665, 2015.

[14] Byung Chul Choi and Young Min Kim. Thermodynamic analysis of a dual loop heat recovery system with trilateral cycle applied to exhaust gases of internal combustion engine for propulsion of the 6800 TEU container ship. *Energy*, 58:404–416, 2013.

[15] H. Ghassemi and H. Zakerdoost. Ship hull-propeller system optimization based on the multi-objective evolutionary algorithm. *Proceedings of the Institution of Mechanical Engineers, Part C: Journal of Mechanical Engineering Science*, 231(1):175–192, 2017.

[16] S. Solem, K. Fagerholt, S.O. Erikstad, and . Patricksson. Optimization of diesel electric machinery system configuration in conceptual ship design. *Journal of Marine Science and Technology (Japan)*, 20(3):406–416, 2015.

[17] F. Baldi, H. Johnson, C. Gabrielii, and K. Andersson. Energy and exergy analysis of ship energy systems - The case study of a chemical tanker. *International Journal of Thermodynamics*, 18(2):82–93, 2015.

[18] G. Theotokatos and G. Livanos. Techno-economical analysis of single pressure exhaust gas waste heat recovery systems in marine propulsion plants. *Proceedings of the Institution of Mechanical Engineers, Part M: Journal of Engineering for the Maritime Environment*, 227(2):83–97, 2012.

[19] Dimitrios T Hountalas, Georgios C Mavropoulos, and Christos Katsanos. Efficiency Optimization of a 2-Stroke Diesel Engine Power Plant Through the Recovery of Exhaust Gas Using a Rankine Cycle. *International Conference on Efficiency, Cost, Optimization, Simulation and Environmental Impact of Energy Systems*, pages 1–17, 2012.

[20] George G. Dimopoulos, Chariklia A. Georgopoulou, and Nikolaos M. P. Kakalis. The introduction of exergy analysis to the thermo-economic

modelling and optimisation of a marine combined cycle system. *Proceedings of the 25th International Conference on Efficiency, Cost, Optimization, Simulation and Environmental Impact Of energy Systems*, pages 221–236, 2012.

[21] Maria E. Mondejar, Fredrik Ahlgren, Marcus Thern, and Magnus Genrup. Quasi-steady state simulation of an organic Rankine cycle for waste heat recovery in a passenger vessel. *Applied Energy*, pages 1–12, 2015.

[22] Anthony F Molland. *The maritime engineering reference book: a guide to ship design, construction and operation.* Elsevier, 2011.

[23] WL McCarthy, WS Peters, and DR Rodger. Marine diesel power plant practices, 1990.

[24] R Balaji and Omar Yaakob. An analysis of shipboard waste heat availability for ballast water treatment. *Journal of Marine Engineering & Technology*, 11(2):15–29, 2012.

[25] Waltteri Salmi, Juha Vanttola, Mia Elg, Maunu Kuosa, and Risto Lahdelma. Using waste heat of ship as energy source for an absorption refrigeration system. *Applied Thermal Engineering*, 115:501–516, 2017.

[26] Gequn Shu, Youcai Liang, Haiqiao Wei, Hua Tian, Jian Zhao, and Lina Liu. A review of waste heat recovery on two-stroke IC engine aboard ships. *Renewable and Sustainable Energy Reviews*, 19:385–401, 2013.

[27] Pierre Marty, Philippe Corrignan, Antoine Gondet, Raphaël Chenouard, and JF Hétet. Modelling of energy flows and fuel consumption on board ships: application to a large modern cruise vessel and comparison with sea monitoring data. In *Proceedings of the 11th International Marine Design Conference, Glasgow, UK*, 2012.

[28] Francesco Baldi, Tuong-Van Nguyen, and Fredrik Ahlgren. The application of process integration to the optimisation of cruise ship energy systems: a case study. In *Proceedings of the 29th International Conference on Efficiency, Cost, Optimization, Simulation and Envirionmental Impact of Energy Systems*, 2016.

[29] Pierre Marty, Jean-François Hétet, David Chalet, and Philippe Corrignan. Exergy analysis of complex ship energy systems. *Entropy*, 18(4):127, 2016.

[30] Turgay Koroglu and Oguz Salim Sogut. Advanced exergy analysis of an organic rankine cycle waste heat recovery system of a marine power plant. *Journal of Thermal Engineering*, 3(2):1136–1148, 2017.

[31] Wes McKinney. Data structures for statistical computing in python. In Stéfan van der Walt and Jarrod Millman, editors, *Proceedings of the 9th Python in Science Conference*, pages 51 – 56, 2010.

[32] L Cohen and WA Fritz. Efficiency determination of marine boilers: Input-output versus heat-loss method. *Journal of Engineering for Power*, 84(1):39–43, 1962.

[33] Vedran Mrzljak, Igor Poljak, and Vedran Medica-Viola. Dual fuel consumption and efficiency of marine steam generators for the propulsion of lng carrier. *Applied Thermal Engineering*, 119:331–346, 2017.

[34] Shan Kuo Wang and Shan K Wang. Handbook of air conditioning and refrigeration. 2000.

[35] Mo Chung and Hwa-Choon Park. Comparison of building energy demand for hotels, hospitals, and offices in korea. *Energy*, 92:383–393, 2015.